RESEARCH PAPER

A Substantial Red and Blue Shift in the Bandgap of Gamma-Alumina Through Controlling the OH/Al Ratio and the Concentration of Sulfate Precursor

M. Ghamari* and M. Ghasemifard

* *ghamari_iust@yahoo.com*

Received: June 2019 Revised: August 2019 Accepted: December 2019

Nanotechnology Lab, Faculty of Engineering, Esfarayen University of Technology, Esfarayen, Iran.

DOI: 10.22068/ijmse.17.2.85

Abstract: *In this research, the dependence of the optical bandgap of nano-meter size gamma-alumina on the OH/Al ratio and concentration of aluminum sulfate is measured through diffuse reflectance spectroscopy (DRS) in the range of 900-1100nm. The samples were prepared via the sol-gel method. The results showed that the bandgap is pH and concentration-dependent but in a different way. The direct bandgap of alumina was determined to be 3.40, 4.37, 3.90, and 3.65 eV for samples prepared at pH 6, 7, 8, and 9, respectively. A decreasing trend was observed with increasing pH (except for pH = 6). The lowering of the bandgap may be associated with the variations in particle size during synthesis due to the quantum size effect. The values of the bandgap increased significantly through increasing concentration (0.1 to 0.3M) from 3.90 to 5.65 eV. The role of concentration in bandgap control is remarkably more than pH.*

Keywords: *Alumina, Bandgap, Concentration, DRS, Tauc relation.*

1. INTRODUCTION

The processing-properties relationship has encouraged researchers towards reaching worthwhile achievements by focusing on more details associated with the cycle of structure-properties-processing-performance in materials science engineering. A lot of research has been carried out to explore the role of processing parameters on different synthesis methods such as sol-gel, gel combustion, hydrothermal, solvothermal, etc[1].

Aluminum oxide (Al_2O_3) as an important dielectric, ceramic, and catalyst has found applications at insulators for electronic usages[2] because of its wide bandgap, low leakage current, and modest value of dielectric constant[3].

According to the literature, it has been observed several ranges of bandgap depending on different experimental parameters and formation conditions[4,5]. Each variable (even those seem not to be important) can affect the formation of the same chemical with different properties, optical features in particular. Of the influencing experimental parameters in wet chemical routes are pH and precursor concentration. As we know, the pH and concentration can render different surface natures and porous characteristics to the aluminum oxide[6]. A lot of studies have been done in the context of mentioned parameters from the point of non-optical properties. However, the lack of research on the effect of pH and concentration on the optical properties in UV-Vis is perceived. In this study, at first, the aluminum oxide is synthesized from aluminum sulfate as an inexpensive precursor and then the optical bandgap is measured from the results of diffuse reflectance spectroscopy (DRS) assisted with mathematical calculations. Finally, the role of pH and concentration on the variation of the bandgap are discussed.

2. EXPERIMENTAL PROCEDURES

All chemicals were prepared from Merck and they were used without further purification. All glassware equipment was cleaned with nitric acid and deionized water before use. In a typical procedure, aluminum sulfate was dissolved into distilled water at room temperature in a beaker and magnetically stirred to obtain a homogeneous solution. Ammonium hydroxide was then added drop-wise until the desired pH values at 6, 7, 8, and 9. Stirring was maintained throughout the

entire experiment. The obtained gel was washed three times with hot deionized water and ethanol to remove the soluble ingredients. The samples then were left in the oven at 90°C for 48 hours and finally calcined in the furnace at 800°C for 4h.

The powders sent for diffuse reflectance spectroscopy (DRS) JASCO model V-670 (Japan) for optical investigations. Two parameters as pH and concentration is going to be discussed therefore the samples with the same concentrations (0.1M) at pH values of 6, 7, 8, and 9 are called 1A6, 1A7, 1A8, and 1A9 and samples with pH 8 and different concentrations of 0.1, 0.2, and 0.3M are called 1A8, 2A8, and 3A8, respectively.

All of the experiments were performed under the same experimental conditions.

The XRD and BET experiments were conducted by XRD PHILIPS model PW1730 with copper lamp 1.54056 angstrom and BET BELSORP-mini II, respectively. FTIR characterizations were performed by using Shimadzu 8400S spectrophotometer in the range of 4000-400 cm^{-1}.

3. RESULTS AND DISCUSSION

3.1. Effect of pH on the Bandgap of Nano Gamma-Alumina

The gamma-alumina samples were optically investigated in the range of 190-1100 nm. Before studying the optical properties, the sample prepared at pH 8 (1A8) was representatively studied via XRD. The pattern obtained can be seen in Fig. 1. The XRD of the sample shows the crystalline nature of 1A8 having a cubic structure (matched with JCPDS 29-0063 card) with a space group of Fm-3m and cell parameters of a=b=c= 3.95 angstroms with perpendicular axes. All the diffracted peaks are assigned to the specific planes and shown in Fig. 1. The researchers recommend that the γ-alumina structure is similar to close-packed oxygen (fcc) lattice with Al ions and vacancies distributed among the tetrahedral and octahedral sites. The smallest structure of γ-Al_2O_3 has 16 Al and 24 O ions in the unit cell derived from the spinel with two cation vacancies at octahedral sites that are farthest from each other[7,8]. The nano-meter size nature of powder can be easily perceived from the broadening of the peaks.

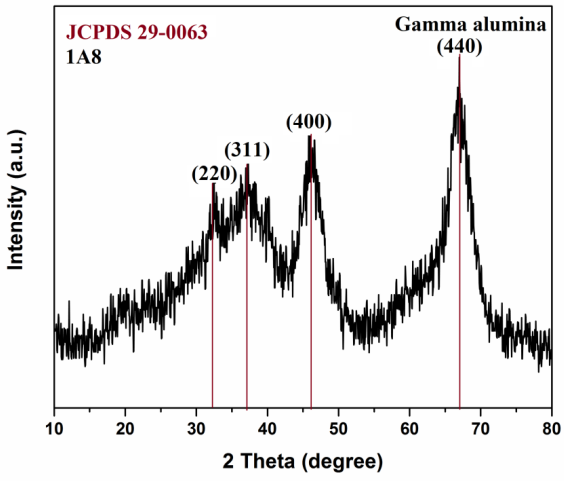

Fig. 1. The XRD pattern of 1A8 calcined at 800 °C.

Fig. 2 shows the FTIR spectra of 1A8 and 3A8 as a representative analysis of samples in 4000-400 cm^{-1}. The shoulder at around 3500 cm^{-1} and the band centered at 1620 cm^{-1} are assigned to the stretching and bending modes of adsorbed water[9]. The bands appeared in the region 400-1000 cm^{-1} belongs to the Al-O vibrations[10] both in tetrahedral and octahedral geometries[11]. Among them the peak at around 750 cm^{-1} may be due to aluminum oxygen stretching vibrations[12]. The peak corresponding to around 1080 cm^{-1} is assigned to Al-O-Al bending stretching vibrations[13]. The absence of the peak of Al-OH at 1074 cm^{-1} indicates the complete transformation of aluminum hydroxides to gamma-alumina during calcination.

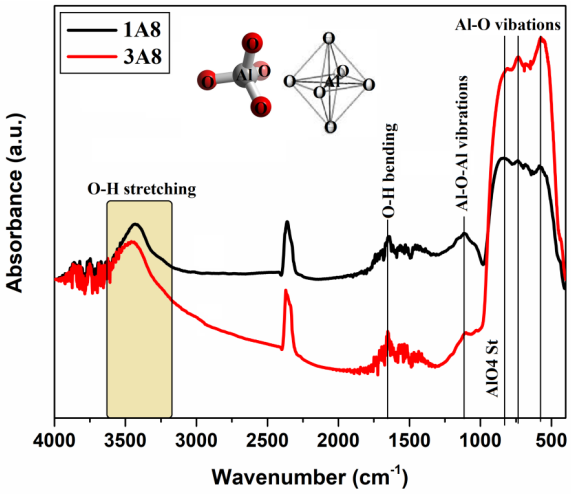

Fig. 2. FTIR spectra of 1A8 and 3A8 calcined at 800°C evaluated in 4000-400 cm^{-1}.

Optical properties of nano-meter size aluminum oxides were recorded based on the results of diffuse reflectance spectroscopy at room temperature at the range of 900-1100 nm, and reflectivity versus wavelengths is shown in Fig. 3.

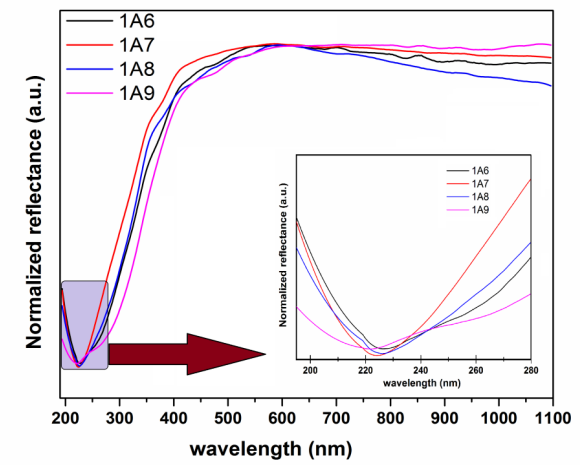

Fig. 3. Normalized reflectance versus wavelength at 900-1100 nm for samples with different pH.

The samples show a strong absorption peak at around 225 nm in the UV region. This can be assigned to the electron transfer from valance to the conduction band of aluminum oxide that can be explained with the mechanism of ligand to central metal charge transfer[14]. The optical energy bandgap is estimated from the Kubelka–Munk method[15], using Tauc relation according to the following equation:

$$(\alpha hv)^{\frac{1}{m}} = c(hv - Eg) \quad (1)$$

The Planck's constant is shown by h, and demonstrates frequency which can be derived from the wavelength. The absorption coefficient, α, determines the effective penetration distance of light with a specific wavelength inside the material and can be calculated from the below relation:

$$\alpha = \frac{(1-r)^2}{2r} \quad , r = \frac{R}{100} \quad (2)$$

The power m attributed to the type of electronic transitions. By plotting vs, E_g can be estimated from the intersection of the tangent and the x-axis. The effect of pH on the E_g values of aluminum oxide is shown in Fig. 4.

Since both direct and indirect bandgaps have been reported for aluminum oxide[16], we can compare the results with the values obtained from mathematical calculations as follows:

$$\frac{d[Ln(\alpha hv)]}{d(hv)} = \frac{m}{hv - Eg} \quad (3)$$

The term $\frac{d[Ln(\alpha hv)]}{d(hv)}$ can be plotted versus and the maximum of the curve gives the value of the E_g with good approximation. The results are shown in Table 1 for comparison.

According to Table 1, the values of direct bandgap energies are in good agreement with the values of column II (without considering m). Therefore the alumina powders have a direct bandgap.

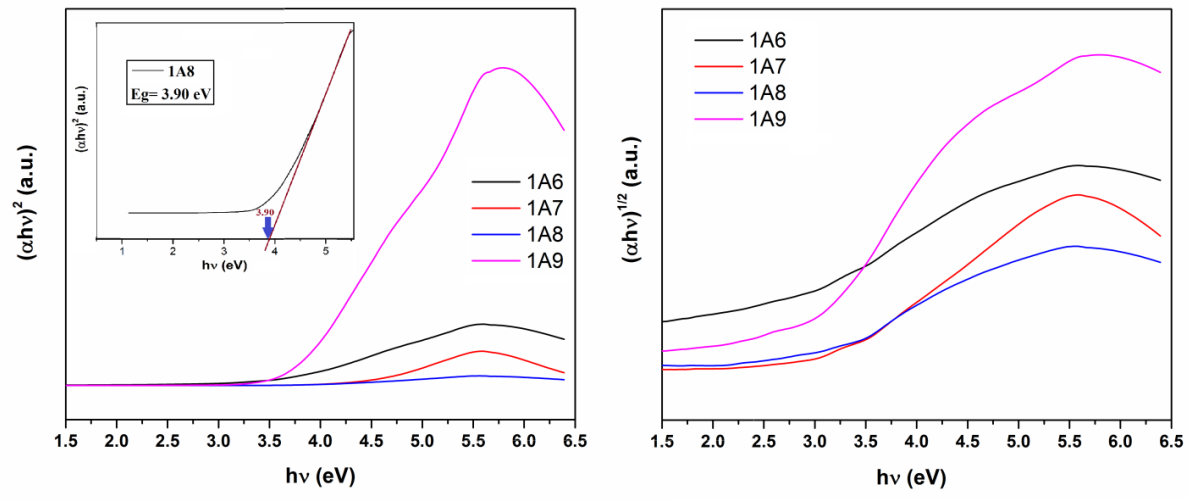

Fig. 4. Effect of pH on calculated bandgaps at direct and indirect states.

Table 1. The obtained energy bandgap values of the samples.

Sample	Bandgap without m	Direct bandgap (eV)	Indirect bandgap (eV)
1A6	3.44	3.40	2.20
1A7	4.40	4.37	2.80
1A8	3.95	3.90	2.67
1A9	6.69	3.65	2.70

As can be seen from Table 1, the bandgaps decreases with increasing pH (except for 1A6) as confirmed by others[17]. The pH is a key parameter with an impact on the properties of nanoparticles in the sol-gel based methods[18]. Notably, the bandgap value depends on the method of synthesis. As can be seen, the optical bandgap in nano alumina is strongly pH-dependent. The effect of pH on the optical bandgap may be discussed in different ways. The first consideration belongs to the fact that the particle size increases with pH rise. Increasing the pH results in the slow nucleation in the solution which in turn creates fewer particles with the bigger size. The increase in particle size as a result of pH variation causes a substantial change in the optical bandgap[19].

According to the quantum size effect, decreasing the size of particles can increase the minimum distance of conduction and valance band due to less marked effects of neighboring atom orbitals resulting in the bandgap increase. This implies that the pH can affect the optical bandgap by changing atomic distances. The sol-gel method is the key factor for the creation of nanoparticles with a specific size. In this way, the size of nanoparticles can be controlled by maintaining important parameters as the rate of addition of the reducing agent like ammonium hydroxide in this case. So the bandgap change occurred due to OH^- concentration during the preparation of alumina nanoparticles.

The second point may be associated with the shift of the bottom of the conduction band depending on alumina formation. The location of the bottom of the conduction band is administrated by the charge transfer from Aluminum atom to the oxygen that depends strongly on the Al atom coordination symmetries which in turn may be affected by pH of the solution[20].

The other point that must be considered relates to the mechanism of particle formation. Anions present at the time of preparation may coprecipitate and change the features from those of pure aluminum hydroxide species. Since the precursor concentration is constant, only the pH (concentration of OH^-) varies. At pH values of less than 8, the neutralization of aluminum sulfate solution with ammonia solution does not result in the formation of pure aluminum hydroxide[21]. Here the precipitate of aluminum hydroxy sulfate is produced which contains some SO_4 groups inside the gel while with increasing pH, the SO_4 groups are replaced with OH groups. The presence of sulfate groups into the structure of aluminum oxide increases the bandgap of the final product. With increasing pH, the sulfate groups disappear and the bandgap decreases afterward. Although the minor values of SO_4 cannot be seen in XRD, it can affect the configuration of electronic orbitals of alumina makes significant changes in optical properties.

3.2. Effect of Precursor Concentration on the Bandgap of Nano Gamma-Alumina

The normalized reflectance of three samples with different concentrations at 900-1100 nm is illustrated in Fig. 5. According to the relations previously discussed, the optical bandgaps (direct and indirect) were calculated and drawn as Fig. 6.

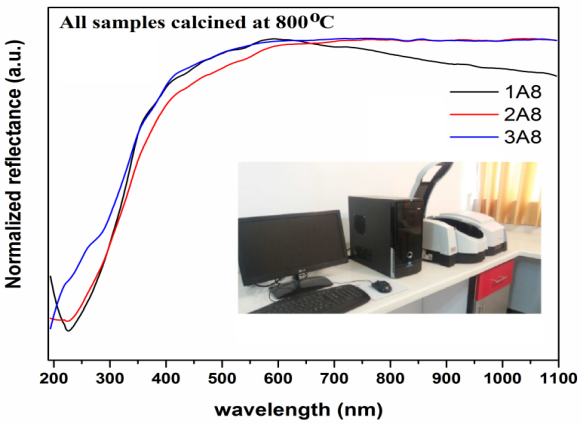

Fig. 5. Normalized reflectance for the samples with different concentrations.

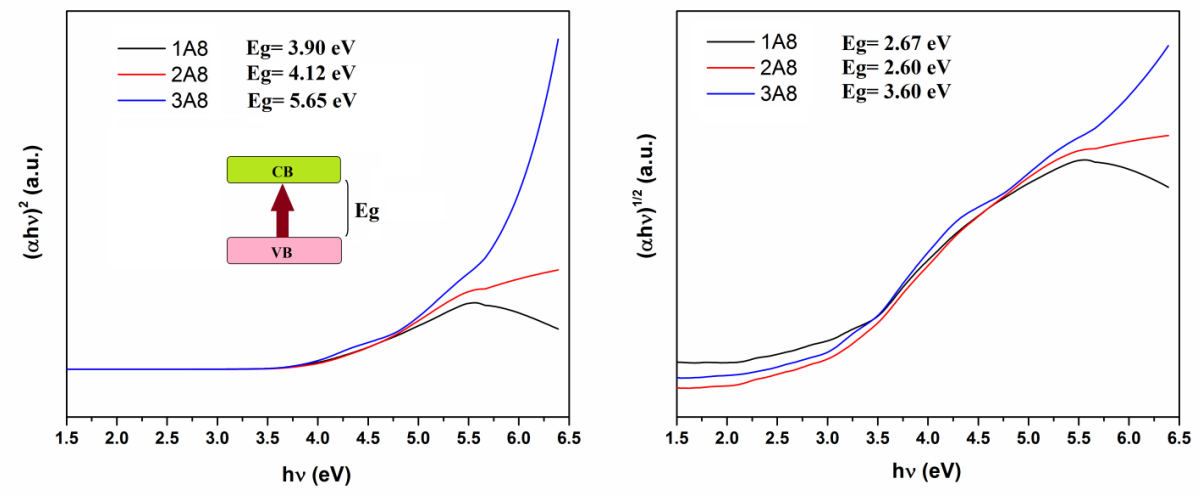

Fig. 6. Effect of concentration on bandgaps at direct and indirect states.

Similarly, we can compare the results of Table 2 (derived from Eq. 3) to find the type of bandgap for the samples with different concentrations.

The bandgap of samples is a direct type. Regarding the results of Table 2, the bandgap of alumina increases significantly with increasing concentration from 0.1 to 0.3M. The number of complexes in aqueous solution increases with increasing concentration at the same water content. On the other hand, the number of sulfate ions increases meaningfully at higher concentrations so that they can affect the stability of complexes which are going to tolerate high temperatures to achieve aluminum oxide. The specific surface area is proportional to the concentration of sulfate precursor. The effect of concentration on the nitrogen adsorption-desorption of powders is shown in Fig. 7. Specific surface area, pore volume values, and pore size distribution of calcined solids at different concentrations are presented in Fig. 6 as inset. Specific surface areas were calculated by the Brunauer-Emmett-Teller(BET) method, while pore volumes were defined by the Barret-Joyner-Halenda (BJH) method.

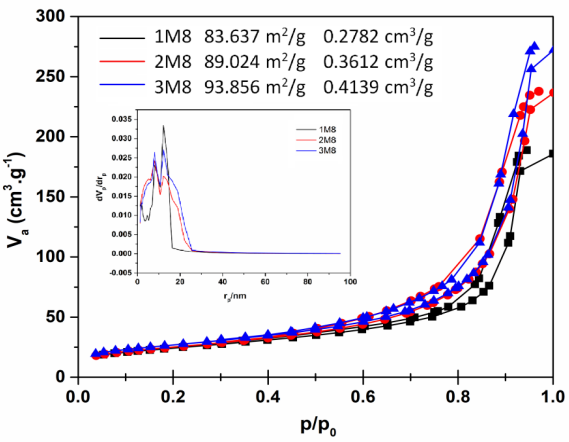

Fig. 7. Effect of concentration on the adsorption-desorption behavior of gamma-alumina.

As can be seen from Fig. 7, the 3M8 possesses the most specific surface area. According to quantum size effect, the high surface area can be equalized to smaller particles results in diminish the effects of neighboring atomic orbitals which in turn can widen the minimum gap between the minimum of conduction and maximum of the valence

Table 2. The obtained energy bandgap values of the samples for different concentrations.

Sample	Bandgap without m	Direct bandgap (eV)	Indirect bandgap (eV)	Others
1A8	3.95	3.90	2.67	4.3[22] 7.6[20] 5.25[23] 7.1[24] 3.9[25]
2A8	4.16	4.12	2.60	
3A8	5.69	5.65	3.60	

band in the direct state. The increasing precursor concentration causes the increase in Al^{3+} ions in solution which in turn raises the possibility of formation of porous aluminum based hydroxides. When the Al ions are high due to concentration increase, the available oxygen in water molecules is not high enough to join the Al-species to form the aluminas in the same water content. Consequently, the smaller complexes are created which possess more specific surface areas like smaller particle size results in increasing the bandgap.

4. CONCLUSION

The aluminum oxide nano-meter size powders have been synthesized by using sol-gel method starting from aluminum sulfate as an inexpensive precursor to seek out the optical bandgap by diffuse reflectance spectroscopy (DRS). The result of XRD on a representative sample depicted the formation of gamma-alumina in accordance with JCPDS 29-0063 card. The effect of OH/Al ratio and concentration on bandgap were explored in the range of 190-1100 nm. Results of DRS and mathematical calculations indicate that that the direct optical bandgap decreases with the increasing pH values (except for the sample prepared at pH = 6) and increases with increasing precursor concentration. The role of concentration on the bandgap variations was found to be more significant than pH.

CONFLICT OF INTEREST

The authors declare that they have no conflict of interest.

REFERENCES

1. Mozaffari, N., Mohammadi, M. R. and Sani, M. A. F., "Development of block copolymer-templated crack-free mesoporous anatase-TiO_2 film: tailoring sol–gel and EISA processing parameters and photovoltaic characteristics", J. Mater. Sci. Mater. Electron. 26, 2015, 1543–1553.
2. Zhang, L., Zhang, Q., Xia, G., Zhou, J., Wang, S., "Low-temperature solution-processed alumina dielectric films for low-voltage organic thin film transistors", J. Mater. Sci. Mater. Electron. 26, 2015, 6639–6646.
3. Esther, A. C. M., Sridhara, N., Sebastian, S. V., Bera, P., Anandan, C., Aruna, S. T., Rangappa, D., Sharma, A. K., Dey, A., "Optical and RF transparent protective alumina thin films", J. Mater. Sci. Mater. Electron. 26, 2015, 9707–9716.
4. Ealet, B., Elyakhloufi, M. H., Gillet, E. and Ricci, M., "Electronic and crystallographic structure of γ-alumina thin films", Thin Solid Films. 250, 1994, 92–100.
5. Toyoda, S., Shinohara, T., Kumigashira, H., Oshima, M., Kato, Y., "Significant increase in conduction band discontinuity due to solid phase epitaxy of Al_2O_3 gate insulator films on GaN semiconductor", Appl. Phys. Lett. 101, 2012, 231607.
6. Sharma, P. K., Varadan, V. V., Varadan, V. K., "A critical role of pH in the colloidal synthesis and phase transformation of nano size α-Al_2O_3 with high surface area", J. Eur. Ceram. Soc. 23, 2003, 659–666.
7. Pinto, H. P., Nieminen, R. M. and Elliott, S. D., "Ab initio study of γ− Al_2O_3 surfaces", Phys. Rev. B. 70, 2004, 125402.
8. Ahuja, R., Osorio-Guillen, J. M., De Almeida, J. S., Holm, B., Ching, W. Y. and Johansson, B., "Electronic and optical properties of γ-Al_2O_3 from ab initio theory", J. Phys. Condens. Matter. 16, 2004, 2891.
9. Tafreshi, M. J. and Khanghah, Z. M., "Infrared spectroscopy studies on sol-gel prepared alumina powders", Mater. Sci. 21, 2015, 28–31.
10. Ghamari, M. and Farzi, G., "The impact of morphology control on the microhardness of PMMA/Boehmite hybrid nanoparticles prepared via facile aqueous one-pot process", J. Sol-Gel Sci. Technol. 2017, 1–10.
11. Urretavizcaya, G., Cavalieri, A. L., Lopez, J. M. P., Sobrados, I., Sanz, J., "Thermal evolution of alumina prepared by the sol-gel technique", J. Mater. Synth. Process. 6, 1998, 1–7.
12. Colomban, P. H., "Raman study of the formation of transition alumina single crystal from protonic β/β″ aluminas", J. Mater. Sci. Lett. 7, 1988, 1324–1326.
13. Parida, K. M., Pradhan, A. C., Das, J., Sahu, N., "Synthesis and characterization of nano-sized porous gamma-alumina by control precipitation method", Mater. Chem. Phys. 113, 2009, 244–248.
14. Ghamari, M., Mirhadi, B., "Composition dependence of spectroscopic properties and transparency of SiO_2-TiO_2-Na_2O glass in 200-1100 nm" , Iran. J. Mater. Sci. Eng. 9, 2012.

15. Vargas, W. E. and Niklasson, G. A., "Applicability conditions of the Kubelka–Munk theory", Appl. Opt. 36, 1997, 5580–5586.
16. Ciraci, S. and Batra, I. P., "Electronic structure of α-alumina and its defect states", Phys. Rev. B. 28, 1983, 982.
17. Amirsalari, A. and Shayesteh, S. F., "Effects of pH and calcination temperature on structural and optical properties of alumina nanoparticles", Superlattices Microstruct. 82, 2015, 507–524.
18. D. H., Kim, Woo, S. I. and Yang, O. B., "Effect of pH in a sol–gel synthesis on the physicochemical properties of Pd–alumina three-way catalyst", Appl. Catal. B. Environ. 26, 2000, 285–289.
19. Mohanraj, V., Jayaprakash, R., Chandrasekaran, J., Robert, R. and Sangaiya, P., "Influence of pH on particle size, band-gap and activation energy of CdS nanoparticles synthesized at constant frequency ultrasonic wave irradiation", Mater. Sci. Semicond. Process. 66, 2017, 131–139.
20. Filatova, E. O. and Konashuk, A. S., "Interpretation of the changing the bandgap of Al_2O_3 depending on its crystalline form: connection with different local symmetries", J. Phys. Chem. C. 119, 2015, 20755–20761.
21. Singh, S. S., "Neutralization of dilute aqueous aluminium sulfate solutions with a base", Can. J. Chem. 47, 1969, 663–667.
22. Costina, I., Franchy and R., "Bandgap of amorphous and well-ordered Al_2O_3 on Ni_3Al (100)", Appl. Phys. Lett. 78, 2001, 4139–4141.
23. Prashanth, P. A., Raveendra, R. S., Hari Krishna, R., Ananda, S., Bhagya, N. P., Nagabhushana, B. M., Lingaraju, K. and Raja Naika, H., "Synthesis, characterizations, antibacterial and photoluminescence studies of solution combustion-derived α-Al_2O_3 nanoparticles", J. Asian Ceram. Soc. 3, 2015, 345–351.
24. Tahir, D., Kwon, H. L., Shin, H. C., Oh, S. K., Kang, H. J., Heo, S., Chung, J. G., Lee, J. C. and Tougaard, S., "Electronic and optical properties of Al_2O_3/SiO_2 thin films grown on Si substrate", J. Phys. D. Appl. Phys. 43, 2010, 255301.
25. Perevalov, T. V., Gritsenko, V. A. and Kaichev, V. V., "Electronic structure of aluminum oxide: ab initio simulations of α and γ phases and comparison with experiment for amorphous films", Eur. Phys. Journal-Applied Phys. 52, 2010.